Separation and Determination of Iron-Containing Proteins via Liquid Chromatography–Particle Beam/Hollow Cathode–Optical Emission Spectroscopy

ARTICLE *in* ANALYTICAL CHEMISTRY · APRIL 2007

Impact Factor: 5.64 · DOI: 10.1021/ac061516p · Source: PubMed

2 AUTHORS, INCLUDING:

R. Kenneth Marcus
Clemson University
202 PUBLICATIONS **3,118** CITATIONS

SEE PROFILE

Anal. Chem. **2007,** *79,* 2402−2411

Separation and Determination of Iron-Containing Proteins via Liquid Chromatography−Particle Beam/Hollow Cathode−Optical Emission Spectroscopy

Tim M. Brewer and R. Kenneth Marcus*

Department of Chemistry, Biosystems Research Complex, Clemson University, Clemson, South Carolina 29634-1905

Presented here is a method for the quantitative determination of iron-containing metalloproteins. Four iron-containing metalloproteins (transferrin, myoglobin, hemoglobin, and cytochrome *c*) were separated by high-performance liquid chromatography (HPLC) and determined through particle beam/hollow cathode−optical emission spectroscopy (PB/HC−OES) by the Fe (I) 371.9 nm optical emission. Parametric optimization of sample introduction, nebulization, and hollow cathode source conditions is performed for the suite of Fe-metalloproteins. Response curves for the Fe (I) emission were obtained under optimized conditions with detection limits for triplicate injections occurring on the nanogram level for iron (~24 ng) with variability of <7% RSD over the concentration range of 0.1−100 μg/mL iron in the metalloproteins. Response curves for S (I) emission yielded similar analytical characteristics. Optical emission detection of the liquid chromatography separations of the iron-containing metalloproteins demonstrates the feasibility of the PB/HC−OES system as a simple element-specific detector for liquid chromatography. The retention times of the four analytes are similar to those determined by UV absorbance (216 nm), demonstrating the ability of the PB interface to preserve the chromatographic integrity of the separation. Additionally, empirical formula calculations based on Fe (I) and S (I) emission response ratios provide a much higher level of specificity than single-element protein determination.

Metal-binding proteins are a major focus of research in biology and medicine due to their functions in connection with transport, storage, and detoxification of trace elements in different organisms.[1−4] These proteins also play a crucial role in a number of key metabolic processes, with one-third of all enzymes being metalloproteins.[5] The metals contained within the protein either fulfill structural functions and/or are essential for the catalytic process. In living organisms, more than a third of cellular proteins have a functional requirement for at least one catalytic or structural metal ion cofactor.[1] In addition to proteins that employ the metals, there are a variety of metal-binding proteins that import, export, and transport metals within the cell, assemble metallocenters, detoxify the cytoplasm, and regulate expression of the various protein factors.[2,3,6] Specifically, iron plays a vital catalytic and structural role in numerous metalloproteins.[7] Under physiological conditions, ferrous ion is highly insoluble and rapidly auto-oxidizes to ferric iron, catalyzing the formation of highly damaging oxygen radicals.[4,8] The importance of iron-containing proteins has necessitated the development of analytical methods for their measurement in biological fluids.[9−12]

There are several methods available for the detection of Fe-metalloproteins. For example, the spectrophotometric detection of metal complexes with 4-(2-pyridylazo)resorcinol (PAR)[13,14] is a rapid, sensitive, and convenient technique that is ubiquitous for quantitative metal analyses at very low (nanomole) levels. However, individual metals are difficult to distinguish using PAR because of the poorly distinguished overlapping spectral characteristics of the chelated metals.[14] Furthermore, the PAR assay is quantitative only when there is complete release of the metal from the denatured proteins into solution; therefore, PAR is not useful for proteins that bind the metals very tightly or in the presence of competing chelators. An assortment of atomic absorption spectrophotometry techniques, including graphite furnace atomic absorption spectrometry (GFAAS)[15] and flame atomic absorption

* To whom correspondence should be addressed. Phone: 864-656-5011. Fax: 864-656-0567. E-mail: marcusr@clemson.edu.

(1) Rusnak, F.; Yu, L.; Mertz, P. *J. Biol. Inorg. Chem.* **1996**, *1*, 388−396.
(2) Outten, F. W.; Outten, C. E.; O'Halloran, T. V. *Bact. Stress Responses* **2000**, 145−157.
(3) Kuchar, J.; Hausinger, R. P. *Chem. Rev.* **2004**, *104*, 509−525.
(4) Buettner, G. R.; Jurkiewicz, B. A. *Radiat. Res.* **1996**, *145*, 532−541.
(5) Garcia, J. S.; Schmidt de Magalhaes, C.; Arruda, M. A. Z. *Talanta* **2006**, *69*, 1−15.
(6) Busenlehner, L. S.; Pennella, M. A.; Giedroc, D. P. *FEMS Microbiol. Rev.* **2003**, *27*, 131−143.
(7) Holm, R. H.; Kennepohl, P.; Solomon, E. I. *Chem. Rev.* **1996**, *96*, 2239−2314.
(8) Wardman, P.; Candeias, L. P. *Radiat. Res.* **1996**, *145*, 523−531.
(9) Whittaker, P.; Wamer, W.; Calvert, R. J. *J. Trace Elem. Exp. Med.* **1992**, *5*, 227−236.
(10) Whittaker, P. G.; Barrett, J. F. R.; Williams, J. G. *J. Anal. At. Spectrom.* **1992**, *7*, 109−114.
(11) Gercken, B.; Barnes, R. M. *Anal. Chem.* **1991**, *63*, 283−287.
(12) Van Landeghem, G. F.; D'Haese, P. C.; Lamberts, L. V.; De Broe, M. E. *Anal. Chem.* **1994**, *66*, 216−222.
(13) Jezorek, J. R.; Freiser, H. *Anal. Chem.* **1979**, *51*, 366−373.
(14) McCall, K. A.; Fierke, C. A. *Anal. Biochem.* **2000**, *284*, 307−315.
(15) Pomazal, K.; Prohaska, C.; Steffan, I. *J. Chromatogr., A* **2002**, *960*, 143−150.

10.1021/ac061516p CCC: $37.00
Published on Web 02/14/2007

spectrometry (FAAS),[16] have been employed for the detection of Fe in proteins. Inductively coupled plasma optical emission spectroscopy (ICP−OES)[17−19] and inductively coupled plasma mass spectrometry (ICP−MS)[20−23] have demonstrated accurate detection of iron-containing metalloproteins. However, as described in subsequent paragraphs, a variety of chemical and spectroscopic interferences can represent additional limitations for both types of ICP analysis. Of perhaps greatest consequence is the incompatibility of the ICP with high levels of organic solvents at flow rates common to reversed-phase liquid chromatography separations. On the other hand, ICP is quite capable of iron excitation and dissociation and is probably the most analytically relevant approach for metal analysis in bulk solution.

Detection of metal constituents alone does not provide complete quantitative or qualitative information about a metalloprotein. Therefore, more information is needed to completely determine metalloprotein species. Obviously, some molecular-based method of detection (e.g., MALDI or electrospray MS) would provide the most unambiguous means of protein determination, but elemental determinations can be used as signatures of target proteins. In order to achieve this, determination of nonmetal elements (in addition to metals) may be employed as a means of gaining more compositional information about the analyte protein. Taken a step further, the ratio of selected elements can provide more definitive species-specific information for protein identification (or at least differentiation). The quantification of analyte-originating nonmetal elements (e.g., H, N, C, and O) is a very difficult task when analyses are performed in open atmosphere environments and in the presence of solvent species. More specifically, the atomic spectroscopy methods presented above suffer from the presence of entrained gases and solute remnants (often from buffer solutions) in the atmospheric pressure sources, limiting the techniques' abilities to determine nonmetals contained within the proteins. This situation is somewhat simplified when the nonmetal element is either sulfur or phosphorus, which are not prominent in the atmosphere (though they are in buffer systems). These elements can be quantified via ICP−OES at levels that are of general utility.[24,25] In the case of ICPMS, possible interferences from molecular ions incorporating nonmetals from the atmosphere can lead to complications in metalloprotein determinations. As a specific example, ICPMS suffers from isobaric/polyatomic interferences for detection of ^{56}Fe species such as the $^{40}Ar^{16}O^+$, decreasing selectivity and sensitivity.[23,26] The use of sector field or collision/reaction cell instruments has overcome many problems with Fe determinations (as a common example) but at a high overhead cost and instrument complexity in comparison to that of OES detection.[23] ICPMS methods have also been described for determinations of nonmetals such as S and P, permitting protein determinations with higher levels of specificity.[27,28] Finally, synchrotron techniques have been utilized for the detailed analysis of metalloproteins, providing quantitative information of iron in liver, but they are not a practical solution for the everyday screening of small amounts of protein.[29,30]

In this laboratory, we have developed the use of a particle beam/hollow cathode−optical emission spectroscopy (PB/HC−OES) source as an on-line, element-specific liquid chromatography detector. The PB/HC−OES system combines the excellent atomization and excitation capabilities of the glow discharge (GD) source[31] with efficient solvent vapor removal of the particle beam,[32,33] thus providing a versatile tool for metal, organometallic, and nonmetal analysis.[34,35] The particle beam interface provides a means of maintaining natural chromatographic characteristics such as retention/elution quality and solvent gradient compatibility with a wide range of solvent polarities and flow rates. The PB interface separates analytes from the liquid mobile phase through a series of three processes: (1) nebulization, (2) desolvation, and (3) momentum separation, ultimately transferring the dry analyte particles into the detection source without mobile phase remnants that cause spectroscopic background. In combination with a simple optical spectrometer system, metal elements have been readily determined using PB/HC−OES on the nanogram/milliliter level, equivalent to the single nanogram absolute mass level.[34−36] More specifically, metals such as copper salts,[37,38] selenium,[39,40] and lead organometallic[36] compounds have been readily determined using this system with low (single part-per-billion) detection limits.

Nonmetal element detection has been illustrated in previous PB/HC−OES works for the analysis of a series of aliphatic amino acids,[35,36] aromatic amino acids,[36] and proteins[41−43] based on the constituent carbon and hydrogen optical emission, with absolute

(16) Ferreira, E. C.; Souza, G. B.; Nogueira, A. R. A. *J. Braz. Chem. Soc.* **2003**, *14*, 329−333.
(17) Silva, F. V.; Lopes, G. S.; Nobrega, J. A.; Souza, G. B.; Nogueira, A. R. A. *Spectrochim. Acta, Part B* **2001**, *56*, 1909−1916.
(18) Szpunar, J. *Analyst* **2000**, *125*, 963−988.
(19) Atanassova, A.; Lam, R.; Zamble, D. B. *Anal. Biochem.* **2004**, *335*, 103−111.
(20) Harrington, C. F.; Elahi, S.; Merson, S. A.; Ponnampalavanar, P. *Anal. Chem.* **2001**, *73*, 4422−4427.
(21) Gomez-Ariza, J. L.; Garcia-Barrera, T.; Lorenzo, F.; Bernal, V.; Villegas, M. J.; Oliveira, V. *Anal. Chim. Acta* **2004**, *524*, 15−22.
(22) del Castillo Busto, M. E.; Montes-Bayon, M.; Blanco-Gonzalez, E.; Meija, J.; Sanz-Medel, A. *Anal. Chem.* **2005**, *77*, 5615−5621.
(23) Hann, S.; Koellensperger, G.; Obinger, C.; Furtmueller, P. G.; Stingeder, G. *J. Anal. At. Spectrom.* **2004**, *19*, 74−79.
(24) Madeddu, B.; Rivoldini, A. *At. Spectrosc.* **1996**, *17*, 148−154.
(25) Tighe, M.; Lockwood, P.; Wilson, S.; Lisle, L. *Commun. Soil Sci. Plant Anal.* **2004**, *35*, 1369−1385.
(26) Petrov, I.; Quetel, C. R. *J. Anal. At. Spectrom.* **2005**, *20*, 1095−1100.
(27) Riondato, J.; Vanhaecke, F.; Moens, L.; Dams, R. *J. Anal. At. Spectrom.* **1997**, *12*, 933−937.
(28) Bandura, D. R.; Ornatsky, O. I.; Liao, L. *J. Anal. At. Spectrom.* **2004**, *19*, 96−100.
(29) Gao, Y.; Chen, C.; Chai, Z.; Zhao, J.; Liu, J.; Zhang, P.; He, W.; Huang, Y. *Analyst* **2002**, *127*, 1700−1704.
(30) Gao, Y.; Chen, C.; Zhang, P.; Chai, Z.; He, W.; Huang, Y. *Anal. Chim. Acta* **2003**, *485*, 131−137.
(31) Marcus, R. K. *Glow Discharge Spectroscopies*; Plenum Press: New York, 1995.
(32) Bellar, T. A.; Behymer, T. D.; Budde, W. L. *J. Am. Soc. Mass Spectrom.* **1990**, *1*, 92−98.
(33) Creaser, C. S.; Stygall, J. W. *Analyst* **1993**, *118*, 1467−1480.
(34) You, J.; Depalma, P. A.; Marcus, R. K. *J. Anal. At. Spectrom.* **1996**, *11*, 483−490.
(35) You, J.; Dempster, M.; Marcus, R. K. *Anal. Chem.* **1997**, *69*, 3419−3426.
(36) Dempster, M.; Marcus, R. K. *J. Anal. At. Spectrom.* **2000**, *15*, 43−48.
(37) Dempster, M.; Davis, W. C.; Marcus, R. K.; Cable-Dunlap, P. R. *J. Anal. At. Spectrom.* **2001**, *16*, 115−121.
(38) You, J.; Fanning, J. C.; Marcus, R. K. *Anal. Chem.* **1994**, *66*, 3916−3924.
(39) Davis, W. C.; Jin, F.; Dempster, M. A.; Robichaud, J. L.; Marcus, R. K. *J. Anal. At. Spectrom.* **2002**, *17*, 99−103.
(40) Jin, F.; Marcus, R. K. *J. Anal. At. Spectrom.* **2003**, *18*, 589−595.
(41) Jin, F.; Hickman, J. J.; Lenghaus, K.; Marcus, R. K. *Anal. Bioanal. Chem.* **2004**, *380*, 204−211.
(42) Jin, F.; Lenghaus, K.; Hickman, J.; Marcus, R. K. *Anal. Chem.* **2003**, *75*, 4801−4810.
(43) Jin, F.; Hickman, J. J.; Lenghaus, K.; Marcus, R. K. *J. Anal. At. Spectrom.* **2004**, *19*, 1199−1205.

detection limits on the single part-per-billion (ng/mL) level. Key to the use of this method was the ability to determine the nonmetal constituents of the amino acids, allowing for more specific distinction of the amino acids from on one another by virtue of their empirical formulas, (e.g., C to H and H to N.) This approach has been used by Brewer and Marcus for the determination of nucleotides through monitoring of phosphorus and carbon emission with detection limits in the single part-per-billion (ng/mL) for P and part-per-trillion (pg/mL) for C.[44] As with the previous experiments the nucleotides were distinguished by their empirical formulas (e.g., P (I)/C (I)) highlighting the technique's ability to provide species-specific information. Recently, total protein determinations have been performed on the PB/HC−OES system through the monitoring of carbon atomic emission resultant from injected bovine serum albumin (BSA).[41−43] Detection limits for BSA were determined down to 15 ng/mL (1 ng absolute) over the concentration range of 0.025−100 μg/mL.

Presented here is further expansion of the capabilities of the PB/HC−OES system for the quantitative and qualitative determination of iron-containing metalloproteins. A suite of iron-containing proteins (cytochrome *c*, transferrin, myoglobin, and hemoglobin) was chosen as a simple test for determinations by iron optical emission responses. Described is a detailed parametric optimization study including sample introduction parameters and discharge operation conditions, with the composite optimized conditions employed for the analytical evaluation. Determinations of the four Fe-metalloproteins included separation by high-performance liquid chromatography (HPLC) and detection by Fe (I) and S (I) optical emission. Furthermore, the feasibility of this method for iron metalloprotein identification is shown via the determination of empirical formulas through the comparison of the measured S (I)/Fe (I) emission intensity ratios to the actual atomic number ratios across the suite of Fe-metalloproteins. Results here demonstrate that species-specific Fe-metalloprotein determinations are achievable using the LC−PB/HC−OES. It is envisioned that the LC−PB/HC−OES system can act as a simple detector for many metalloproteins systems.

EXPERIMENTAL SECTION

Sample Preparation and Solution Delivery. High-purity (~10^{18} MΩ/cm) Barnstead Nanopure (Dubuque, IA) water and acetonitrile (Fisher Scientific, Fair Lawn, NJ) were used for sample preparation and the mobile phase solutions. Primary stock solutions (80 mg/mL) of individual Fe-metalloproteins (transferrin, myoglobin, cytochrome *c*, and hemoglobin, Sigma-Aldrich, St. Louis, MO) were prepared in Nanopure water with 0.1% HPLC-grade trifluoroacetic acid (TFA).

The chromatographic system consisted of a Waters (Milford, MA) model 600E high-performance liquid chromatography pump with a six-port Rheodyne injection valve (model 7520, Rheodyne Inc., Cotati, CA) fitted with a 50 μL injection loop. Separations of the Fe-metalloproteins were performed on a capillary-channeled polymer (C-CP) fiber reversed-phase column as described in the following sections at a flow rate of 2.0 mL/min.[45] A Waters 2487 dual wavelength absorbance detector was employed at 216 nm. The data for the chromatogram (absorbance vs elution time) was generated by Millennium 32 Chromatography Manager and further processed in the form of Microsoft (Redmond, WA) Excel files.

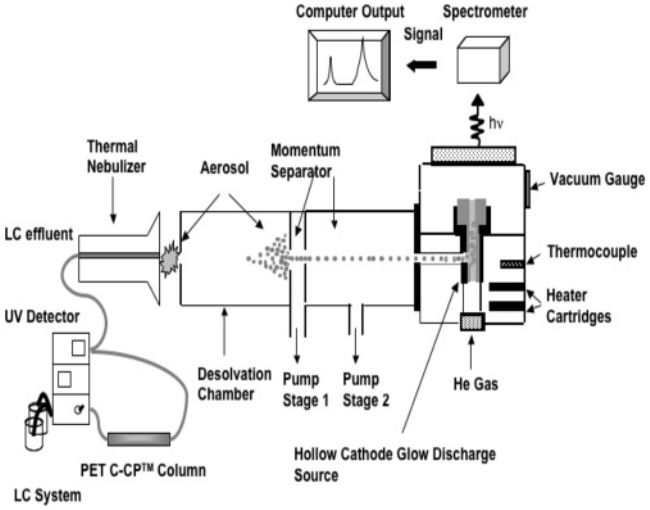

Figure 1. Diagrammatic representation of the HPLC−PB/HC−OES system.

Chromatographic Columns. Polyester (PET) C-CP fibers of 50 μm nominal diameter were obtained from School of Material Science and Engineering, Clemson University and prepared in a manner that was similar to previous methods.[45−48] The fibers were manually wound onto a circular frame to accumulate enough strands to tightly fill the stainless cell column (4.6 mm i.d. × 150 mm length). The fiber loop was pulled through the tubing using a plastic monofilament (4 lb test) and passing it through the column. The initial length of the fibers was such that the fiber ends extended past both ends of the tubing, with the general alignment being longitudinally parallel. The excess fiber was trimmed flush with the column ends. The column ends were sealed with a 0.75 mm thick, 6.35 mm diameter frits (2 μm pores) and completed with column end fittings from Valco Instruments Co. Inc. (Houston, TX). The columns were flushed with ACS-grade acetonitrile and Nanopure water to remove any residual surfactant. Prior to each run, the C-CP fiber column was washed with 100% ACN containing 0.06% (v/v) TFA until the baseline absorbance response was stable, then equilibrated with 100% Nanopure water containing 0.1% (v/v) TFA.

Hollow Cathode Glow Discharge Source. The PB/HC−OES source instrumentation, shown in Figure 1, is basically the same design as applied in previous studies.[44] The HC is mounted at the center of a stainless steel "thermoblock", which serves as the (grounded) anode of the GD circuit. The source vacuum port, discharge gas inlet, pressure gauge, electrical feedthroughs, and heating components are also located in the thermoblock. The entire thermoblock is heated for efficient sample vaporization and atomization by a pair of cartridge heaters (model SC 2515, Scientific Instrument Services, Ringoes, NJ), with the block temperature monitored by a W−Re thermocouple. The gas

(44) Brewer, T. M.; Fernandez, B.; Marcus, R. K. *J. Anal. At. Spectrom.* **2005**, *20*, 924−931.
(45) Nelson Dwella, K.; Marcus, R. K. *J. Chromatogr. Sci.* **2003**, *41*, 475−479.
(46) Marcus, R. K.; Davis, W. C.; Knippel, B. C.; LaMotte, L.; Hill, T. A.; Perahia, D.; Jenkins, J. D. *J. Chromatogr., A* **2003**, *986*, 17−31.
(47) Stanelle, R. D.; Mignanelli, M.; Brown, P.; Marcus, R. K. *Anal. Bioanal. Chem.* **2006**, *384*, 250−258.
(48) Stanelle, R. D.; Sander, L. C.; Marcus, R. K. *J. Chromatogr., A* **2005**, *1100*, 68−75.

pressure within the GD source is monitored by a Pirani-type vacuum gauge (VRC model 912011, Pittsburgh, PA). The HC discharge is powered by a Bertan (Hicksville, NY) model 915-1N supply, operating in the constant-current mode over the range of 20−80 mA.

Helium is used as the discharge gas in this study. The high-lying He metastable-atom levels (19.77 and 20.55 eV) are able to provide energy for molecular dissociation as well as excite the analyte atoms. In addition, the high-energy electron populations produced in the He plasma more efficiently dissociate molecular species as well as contributing to the excitation of analytes such as Fe and S.[49]

Particle Beam Interface. A Thermabeam (Extrel Corporation, Pittsburgh, PA) particle beam LC/MS interface is employed to couple the liquid flow with the HC GD source. The interface consists of a thermoconcentric nebulizer, a heated spray chamber, and a two-stage momentum separator. The liquid sample is introduced via the HPLC flow into a fused-silica capillary (110 μm i.d.) mounted within a stainless steel tube (1.6 mm o.d.). A dc potential difference placed across the two ends of the stainless steel tube results in resistive heating, adding a thermal component to the aerosol formation to help desolvate the liquid drops. A coaxial flow of helium gas between the central fused-silica capillary and outer stainless steel tubing serves as a sheath gas facilitating heat conduction into the capillary and to break up the liquid at the capillary tip (i.e., pneumatic nebulization). The resultant fine aerosol is directed into a 35 mm diameter, 110 mm long steel spray chamber wrapped in electrical heating tape. The operating temperature of the chamber was fixed at 150 °C. The separation of the aerosol (a mixture of He gas and analyte, carrier, and solvent) is achieved by a two-stage momentum separator, which skims away the relatively low-mass nebulizer gas (He) and eluent solvent vapors, leaving dry analyte particles on the scale of 1−10 μm.[33,50] The resultant beam of dry particles enters the heated HC discharge volume for subsequent vaporization, atomization, and excitation.

Optical Spectrometer and Data Acquisition. Optical emission from the HC discharge is sampled using a plano−convex fused-silica lens such that the image of the excitation region is focused at a ratio of ~1:1 on the entrance slit of the spectrometer. A nitrogen-purged 1.0 m Czerny−Turner monochromator equipped with a 3600 grooves/mm holographic grating (Jobin−Yvon 38, Longjumeau, France) is employed for optical monitoring. Atomic emission signals, detected by a photomultiplier tube (PMT) (Hamamatsu model R955, Bridgewater, NJ) are then converted into voltage signals with a digital current meter. A personal computer is employed to record the output of the voltage meter via a National Instruments (Austin, TX) PCI-6221 interface board. An $X-Y$ recorder-type program within National Instruments LabView 7.1 software environment has been developed for acquisition of the optical responses. The data is processed in the form of Microsoft (Redmond, WA) Excel files. Peak (single-wavelength) intensities are reported for the case of studying the role of solvent composition on the spectral background. Transient peak areas are calculated by integrating the total signal from the peak starting point, after subtracting the background for an analogous time frame with smoothing of the data points. These values are self-consistent within each study but vary across experiments involving a given analyte element. In addition they cannot be compared between the different analyte species as PMT voltages, etc., are not held constant.

RESULTS AND DISCUSSION

Effect of Discharge Conditions on the Fe (I) Responses. Spectrochemical (elemental) analysis of metalloproteins is based on the assumption that the conversion of the metal-containing analyte molecules to free atoms is quantitative. This is challenging for proteins primarily due to the folding of the proteins which "entraps" the metal. Previous work has shown that vaporization from the HC walls is the primary means of generating gas-phase molecules and fragments.[37] Further dissociation of molecular species may occur during the vaporization process or through collisions with electrons, ions, and neutral particles in the gas phase.[31] As with conventional GD sources employed in direct solids analysis,[51,52] optimum discharge conditions need to be determined through variation of the discharge current and the discharge gas (helium) pressure while monitoring the analyte emission response. It has generally been found with other analyte systems (i.e., amino acids and proteins) that the optimum HC−OES response occurs at high currents and low gas pressures.[36,42,43] In general terms, this reflects the extent of electron impact excitation and Penning collision processes.

Figure 2a depicts the response of the Fe (I) 371.9 nm emission intensity, for 50 μL injections of 80 mg/mL myoglobin, to increases in discharge current at a fixed pressure of 2 Torr of He. The proportional increase with discharge current reflects the fact that the extent of sample excitation increases with the electron number density.[53,54] Higher discharge currents result in higher free electron density, resulting in larger extents of excitation and vice versa for low discharge current. Above 60 mA, a decrease in emission intensity is observed, which is a similar result to previous experiments.[44] This phenomenon is possibly due to self-absorption, as an increase in current can increase access to nonemitting pathways. Additionally, increased current can better populate higher-lying states that do not relax through the specific monitored transition. Secondary discharges, common in some GD sources, have been ruled out as a means of draining energy at high currents in this case as there is no electrical or physical evidence of such. More unlikely, though possible, is the potential for greater extents of postatomization chemical reactions, decreasing the free atom population. It should be noted that each of the Fe-metalloproteins studied elicited that same response. As such, a discharge of 60 mA was used for the remainder of the Fe-metalloprotein analyses described herein.

Discharge gas pressure plays an important role in collisional processes as increases in pressure increase the gas-phase collision frequency.[55] As such, high gas pressures would tend to increase the efficiency of molecular species dissociation if this is a

(49) Christopher, S. J.; Hartenstein, M. L.; Marcus, R. K.; Belkin, M.; Caruso, J. A. *Spectrochim. Acta, Part B* **1998**, *53*, 1181−1196.
(50) Willoughby, R. C.; Browner, R. F. *Anal. Chem.* **1984**, *56*, 2625−2631.
(51) Anfone, A. B.; Marcus, R. K. *J. Anal. At. Spectrom.* **2001**, *16*, 506−513.
(52) Luesaiwong, W.; Marcus, R. K. *Microchem. J.* **2003**, *74*, 59−73.
(53) Brackett, J. M.; Mitchell, J. C.; Vickers, T. J. *Appl. Spectrosc.* **1984**, *38*, 136−140.
(54) Borodin, V. S.; Kagan, Y. M. *Sov. Phys. Tech. Phys.* **1966**, *11*, 131.
(55) Marcus, R. K.; Broekaert, J. A. C. *Glow Discharge Plasmas in Analytical Spectroscopy*; John Wiley & Sons: Chichester, U.K., 2003.

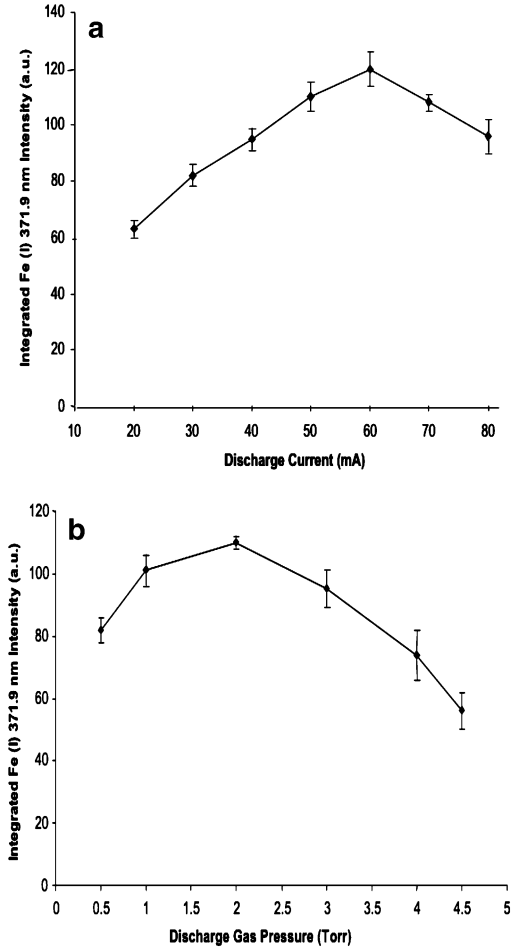

Figure 2. Effect of discharge conditions on Fe (I) 371.9 nm emission intensity for myoglobin. (a) Role of discharge current and (b) role of He discharge gas pressure. Solvent = 25:75 H_2O/ACN, injection volume = 50 μL, flow rate = 2 mL/min, nebulizer tip temp = 100 °C, nebulizer gas flow rate = ~800 mL/min, HC block temp = 250 °C.

prominent occurrence. Conversely, electron energies decrease along with discharge maintenance voltage because of increased gas density.[55] Therefore, the net excitation efficiency decreases when electron impact is the primary excitation mechanism. These counteracting processes are demonstrated in Figure 2b for injections of the 80 mg/mL myoglobin (200 μg/mL iron) at a fixed discharge current of 60 mA. The Fe (I) emission intensity response passes through a maximum at ~2 Torr as the He discharge gas pressure is increased from ~0.5 to 4.5 Torr. This response is interpreted as a combination of the above-described phenomena, where increased pressure improves gas-phase dissociation, but ultimately begins to suppress electron impact energetics. Previous results in this lab have shown similar results with an optimal signal achieved at a pressure of 2 Torr.[44] Here again, each member of the suite of Fe-metalloproteins showed similar response as the myoglobin. Thus, a pressure of 2.0 Torr of He was chosen as the operating pressure for the remainder of these studies.

Effect of Nebulizer and Hollow Cathode Block Temperatures on Analyte Responses. As in other spectrochemical techniques where nebulization is employed, the effect of delivery (i.e., solution flow) rate on the overall sample introduction efficiency and plasma performance is of concern.[56] The nebulizer

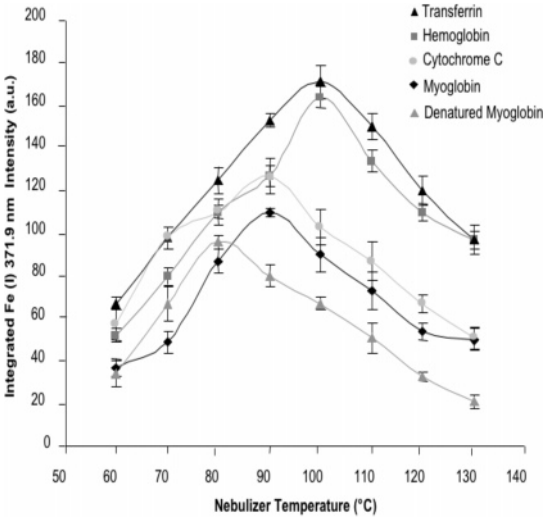

Figure 3. Effect of nebulizer tip temperature on Fe (I) 371.9 nm emission intensity for triplicate injections of 200 μg/mL Fe in transferrin, hemoglobin, cytochrome *c*, myoglobin, and denatured myoglobin. Solvent = 25:75 H_2O/ACN, injection volume = 50 μL, flow rate = 2 mL/min, nebulizer gas flow rate = ~800 mL/min, HC block temp = 235 °C, source pressure = 2 Torr of He, discharge current = 60 mA.

Table 1. Molecular Weight and Stoichiometric Content of Analyzed Metalloproteins

metalloprotein	mol wt (Da)	iron atoms per molecule	sulfur-containing amino acids per molecule	stoichiometric sulfur/metal ratio
cytochrome *c*	11702	1 Fe	6	6
myoglobin	16954	1 Fe	5	5
hemoglobin	61968	4 Fe	16	4
transferrin	79550	2 Fe	50	25

temperature of the thermobeam device plays a crucial role in the overall performance of the particle beam sample introduction system. If the temperature is too low, the analyte-containing solution will not be efficiently nebulized, resulting in gravitational losses of large droplets in the spray chamber. On the other hand, an excessively high temperature can result in desolvation of analyte particles inside the nebulizer head, eventually clogging the fused-silica capillary. These considerations for nebulization are magnified for the suite of Fe-metalloproteins studied due to their large molecular weights (Table 1), making them more susceptible to pyrolysis due to their carbon-rich nature. Figure 3 depicts the response of the Fe (I) 371.9 nm emission as a function of the nebulizer tip temperature for the suite of iron-containing metalloproteins. As can be seen for the larger proteins, hemoglobin and transferrin, 100 °C gave an optimal signal, while for the smaller proteins, myoglobin and cytochrome *c*, 90 °C gave an optimal signal. This difference in optimal temperatures for larger and smaller proteins was expected because increased thermal energy is required to aerosolize the metalloproteins based on their relative masses. Results shown here varied from those of previous PB/HC−OES experiments for inorganic metals[34] and total protein[42] analysis where a nebulizer tip temperature of 220 °C yielded

(56) Montaser, A., Golightly, D. W., Eds. *Inductively Coupled Plasmas in Analytical Atomic Spectrometry*; Wiley-VCH: New York, 1987.

an optimal signal. This difference is attributed to the fact that the proteins studied here are larger and higher temperatures would likely cause denaturation and surface adsorption (as described below), leading to clogging. On the basis of the results of these nebulizer optimization studies a compromise tip temperature of 95 °C was employed for the remainder of the experiments involving the suite of Fe-metalloproteins. While it would be desirable that each protein would show the same response to nebulizer temperature changes, it is perhaps surprising (given the diversity in proteins) that none of the proteins suffers greater than an ~20% sacrifice from their optimum response by operation at 95 °C.

The biological activity of a protein is closely linked to its native structure, which is retained only if critical factors such as temperature, pH, and solvent identity are kept within narrow limits. Outside of these bounds, the overall structure and conformation of the protein will change, typically resulting in unfolding of the protein, called denaturation. A conformational change can result in more or less thermal energy needed to effectively nebulize and dissociate the iron within the protein using the PB/HC−OES system. Therefore, the effect of denaturating of proteins on the metal analyte emission response also needs to be accounted for in this study. Figure 3 also shows the response of myoglobin that has been denatured in 6 M guanine. Following denaturation, a decrease in the optimal nebulizer temperature to ~80 °C is observed, which is attributed to a conformation change in the protein exposing more of the protein core as well as making it more easily desolvated. Additionally, a decrease in Fe (I) response is seen, which may seem counter intuitive given the fact that the iron is more available following denaturation. There are a couple of possibilities that could account for the overall decrease in emission intensity: (1) an increase in hydrodynamic volume is realized which in turn causes pyrolyization of the protein onto the silica capillary walls decreasing intensity or (2) interactions between the denatured myoglobin and the exposed silanol groups on the silica nebulizer tubing are increased because more of the metalloprotein core is exposed, decreasing the intensities. Pyrolysis and/or increased interactions with the silica capillary tubing were clearly evident by frequent clogging of the nebulizer upon injection of the denatured metalloprotein. All of the Fe-metalloproteins studied showed similar results to those of myoglobin in both the native and denatured states.

The temperature of the HC walls has a crucial effect on the response of the analyte atoms/molecules entering into the plasma of the HC.[34] There are three modes of atomization that exist in HC glow discharges depending on the surface temperature. If the temperature of the HC source is sufficiently low, cathodic sputtering is the major mechanism for atomization. When the HC source has modest temperature (~100 °C) both cathodic sputtering and selective vaporization of volatile compounds may occur. At high HC temperatures (>100 °C) thermal volatilization predominately contributes to the atomization process.[55] Early research in this group involving PB/GD clearly indicated the need to provide a thermal component for sample atomization, beyond the simple cathodic sputtering process.[34,37,57] Dempster and co-workers demonstrated the presence of species-specific threshold temperatures for a number of copper salts, above which the emission intensity increased owning to increased vaporization/atomization efficiency.[37] Optimal values for the HC using copper salts were found between 250 and 350 °C. However, at excessively high HC temperatures, the vaporization efficiency decreased due to pyrolysis of the analytes on the heated HC wall.[37] Certainly, the latter process is of greater concern for the carbon-rich metalloproteins in this study.

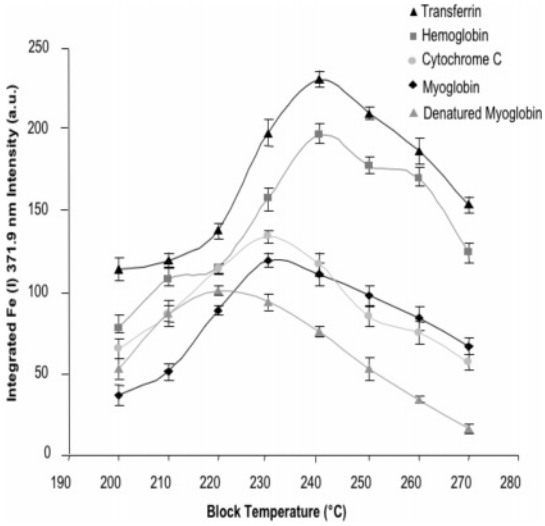

Figure 4. Effect of HC block temperature on Fe (I) 371.9 nm emission intensity for triplicate injection of 200 μg/mL Fe in transferrin, hemoglobin, cytochrome *c*, myoglobin, and denatured myoglobin. Solvent = 25:75 H_2O/ACN, injection volume = 50 μL, flow rate = 2 mL/min, nebulizer tip temp = 95 °C, nebulizer gas flow rate = ~800 mL/min, source pressure = 2 Torr of He, discharge current = 60 mA.

The effect of source block temperature on the resultant Fe (I) 371.9 nm emission response for the suite of Fe-metalloproteins was determined across the temperature range of 200−270 °C, as shown in Figure 4. Clearly seen is the optimal Fe (I) emission response at an HC temperature of 240 °C for transferrin and hemoglobin, while at 230 °C the optimal response for myoglobin and cytochrome *c* was obtained; this again relates the metalloprotein's molecular weight and the thermal energy needed to vaporize and dissociate the individual metalloproteins. The observed responses at the lower temperatures (200−220 °C) suggest there is not enough heat available for efficient vaporization. Above 240 °C it is possible that the Fe-metalloproteins form larger molecular aggregates, which deposit on the HC walls and eventually undergo pyrolysis. This was evident following cleaning of the instrument as well as during operation, where an increase in current was required following operation at 240 °C and above for extended periods of time. Once pyrolyzed, the proteins have a greatly reduced volatility and in fact would be much more difficult to dissociate if they were to enter the gas phase.

The response of the denatured myoglobin is also shown in Figure 4. A decrease in the optimal HC temperature and a decrease in emission intensity following denaturation is seen here, as was the case for the study of the role of the nebulizer tip temperature. When the protein is denatured, a decrease in the optimum vaporization temperature to ~220 °C is seen, reflecting the greater ease of dissociation. The overall decrease in iron emission response is consistent with the interactions of the denatured myoglobin within the nebulizer capillary. All of the other

(57) You, J.; Dempster, M. A.; Marcus, R. K. *J. Anal. At. Spectrom.* **1997**, *12*, 807−815.

Table 2. Fe (I) 371.9 nm Response Function Characteristics for the Suite of Metalloproteins

metalloprotein	response function	correlation (R^2)	protein LOD (μg/mL)	Fe LOD (μg/mL)	absolute mass Fe (ng)
cytochrome *c*	$y = 1.68x - 1.11$	0.997	230	0.57	28.5
myoglobin	$y = 1.65x - 0.68$	0.998	320	0.79	39.5
hemoglobin	$y = 1.59x - 0.06$	0.996	430	1.1	55.0
transferrin	$y = 2.15x - 0.34$	0.998	188	0.47	23.5

Table 3. S (I) 180.7 nm Response Function Characteristics for the Suite of Metalloproteins

metalloprotein	response function	correlation (R^2)	protein LOD (μg/mL)	S LOD (μg/mL)	absolute mass S (ng)
cytochrome *c*	$y = 2.96x + 3.04$	0.998	43	0.12	6.0
myoglobin	$y = 2.46x + 1.99$	0.989	98	0.29	14
hemoglobin	$y = 8.51x - 1.34$	0.987	31	0.81	41
transferrin	$y = 25.3x + 4.09$	0.999	4.1	0.26	13

proteins studied showed similar responses to myoglobin when denatured. On the basis of the results of these studies, a compromise block temperature of 235 °C was employed for the remainder of the experiments. While it would be desirable that each protein would show the same response to vaporization temperature changes, it is again perhaps surprising that none of the proteins suffers greater than an ~20% sacrifice in response at the chosen compromise vaporization temperature.

Analytical Figures of Merit. Having optimized the PB/HC−OES system parameters, general figures of merit were determined for the suite of Fe-metalloproteins. Analytical response curves were obtained from the Fe (I) 371.9 nm emission for each of the test proteins. The metalloprotein concentrations ranged from 0.1 to 100 μg/mL of iron in each of the respective metalloproteins. The variability in Fe (I) response across each of the concentrations was <7% RSD. Table 2 presents the statistical figures of merit derived from the calibration functions. The myoglobin, cytochrome *c*, and hemoglobin exhibit very similar sensitivities (Table 2), which is to be expected because they have similar binding structures, where iron is in the form of a heme group and held in a heterocyclic ring. The Fe (I) response for transferrin demonstrates higher sensitivity because the binding sites for iron are not coordinated in a heterocyclic ring, as in the case for the other metalloproteins studied, and are thus more readily dissociated.[58,59] Iron in transferrin is found in receptor lobes in the form of a bridging ligand between the metal and the protein protruding from the backbone of the protein.[56,57] We are unfamiliar with any analogous studies in ICP−OES/MS wherein the response functions of different proteins are compared. On the basis of the linear regression statistics of the response curves and the use of triplicate solvent blank injections, limits of detection ($3\sigma_{blank}/m$) for iron ranged from 0.47 to 1.1 μg/mL. In each case, a linear dependence with a high degree of correlation (R^2) exists, clearly demonstrating the technique's ability to determine iron in metalloproteins. The LODs in these iron-containing metalloproteins are comparable to previous results for total protein determination using PB/HC−OES[41−43] and are very comparable to those for metal elements in proteins by ICP−OES.[17,19,60,61]

In order for the PB/HC−OES technique's validity to be verified for protein-specific determinations via empirical formulas, stoichiometric relationships must be realized for other elements. One of the major components of proteins is sulfur, which provides structural support for the protein in the form of a disulfide bond.[62] It also serves as minor constituent of fats, body fluids, and skeletal minerals.[62] Detection and determination of sulfur is easily achieved using PB/HC−OES due to the inert atmosphere. Analytical response curves for S (I) 180.7 nm emission resultant from the test proteins are shown in Table 3 for metalloprotein concentrations ranging from 0.1 to 100 μg/mL of sulfur in each metalloprotein, representing a range of ~2.5 μg/mL to 6.1 mg/mL of proteins. The variability for all of the sets of triplicate injections is in the range of 3−6% RSD. In the ideal case where protein dissociation occurred with unit efficiency, there would be no differences in response functions between the proteins. As in the case of the Fe (I) responses, the difference in slopes (sensitivity) for each of the metalloproteins is likely related to the accessibility of the sulfur atoms within the proteins for release upon vaporization, which varies far more greatly than for iron. For example, the relative number of sulfurs involved in disulfide linkages varies greatly from protein to protein. Linear regression statistics of the response curves and use of triplicate solvent blank injections yielded S limits of detection ranging from 0.26 μg/mL for transferrin to 0.81 μg/mL for hemoglobin in the suite of metalloproteins shown in Table 3. Lower limits of detection were achieved for sulfur because the spectral background/noise levels are far lower than those at the Fe (I) wavelength.

Separation and Determination of Fe-Metalloproteins. In order to realize the complete speciation analysis of Fe-metalloproteins via PB/HC−OES, a high-performance liquid chromatography (HPLC) separation of the analytes is required. Previous work in this laboratory has shown that a fast reversed-phased separation of holo-transferrin, cytochrome *c*, ribonulease A, and myoglobin is possible using polyester (PET) capillary-channeled

(58) Cheng, Y.; Zak, O.; Aisen, P.; Harrison, S. C.; Walz, T. *Cell* **2004**, *116*, 565−576.
(59) Aisen, P. *Met. Ions Biol. Syst.* **1998**, *35*, 585−631.
(60) Pomazal, K.; Prohaska, C.; Steffan, I.; Reich, G.; Huber, J. F. K. *Analyst* **1999**, *124*, 657−663.
(61) Caroli, S.; La Torre, F.; Petrucci, F.; Senofonte, O.; Violante, N. *Spectroscopy* **1993**, *8*, 46−50.
(62) Mikkelsen, S. R.; Corton, E. *Bioanalytical Chemistry*; John Wiley & Sons, Inc.: Hoboken, NJ, 2004.

polymer (C-CP) fiber stationary phases.[63] Therefore, a PET fiber column was employed for the separation of a mixture (~1 mg/mL protein) of myoglobin, hemoglobin, transferrin, and cytochrome *c*. A loading time of 2.5 min with Nanopure water was employed prior to initiation of the gradient. A gradient was applied going from 100:0 (water/acetonitrile) mixture to 25:75 composition over the 2.5−10 min period; as such, the total elution time is less than 10 min. This demonstrates one of the primary advantages of the PB/HC−OES approach for speciation analysis as gradient elution with a 75% ACN mobile phase composition and flow rate of 2 mL/min cannot be coupled directly into an ICP source.

Figure 5a shows the resulting chromatogram for a 50 μL injection of the compounds employing UV absorbance detection at 216 nm. One of the more important aspects of using the LC−PB combination, in general, is the ability to develop separation strategies independently, without regard to possible incompatibility with the detection system.[33] With the use of the PB, gradient flows are not particularly problematic as the solvent vapors are pumped away in the interface. The corresponding separation with PB/HC−OES detection at the Fe (I) 371.9 nm and S (I) 180.7 nm transitions are shown if Figure 5, parts b and c, respectively, demonstrating the ability of the PB interface to preserve the chromatographic integrity of the separation. Collection of sulfur and iron was not done simultaneously because only a monochromator is currently available for detection.

The transients obtained by OES appear just slightly later than for UV due to the difference in flow distance to the PB nebulizer, though the relative peak elution times (i.e., the selectivity and resolution) are not affected. The slight broadening observed in the OES chromatogram is likely due to lateral diffusion over the course of the longer transit distance. Differences between the two OES responses reflect the fact that the chromatograms are derived from two different injections, one at each element's optical transition, taken under different PMT conditions and thus not having the same signal-to-noise and background correction quality. Clearly, such variations would diminish in the case of simultaneous, multielement monitoring.

One important point that must be addressed in any form of gradient elution chromatography is the effect of gradient composition on the individual analyte response characteristics. Variations in response are common in almost all forms of detection, including optical absorption, optical emission, and mass spectrometry. In the case of the LC−PB/HC−OES technique, changes in solvent composition could effect the nebulization efficiency, the desolvation efficiency, and perhaps lead to variations in spectral background. It is not likely that solvent composition would effect the molecular dissociation or analyte excitation processes. Figure 6 depicts the Fe (I) 371.9 nm responses for 50 μL injections of 200 μg/mL Fe in myoglobin as a function of discharge current for solvent compositions ranging from 100:0 to 25:75 H_2O/ACN. Overall, the changes in solvent composition have a relatively small effect on the product Fe (I) emission. As can be seen in the figure, the changes with respect to discharge current parallel each other regardless of the solvent composition. In every case, the 50:50 H_2O/ACN solvent yields the highest response. One might have expected, on the basis of volatility issues, that the responses for the pure aqueous mobile phase would be the lowest and the one with the greatest organic content to be the highest, but this is not the case. It is likely that the higher organic content may in fact nebulize too well, yielding small droplets and resulting particles, which may not pass efficiently through the momentum separator. As was seen in Figure 2a, the greatest Fe (I) response is seen at a discharge current of 60 mA. At this current, the total variation in the responses across the range of solvent compositions (Figure 6) is less than 25%. A similar study of the role of solvent

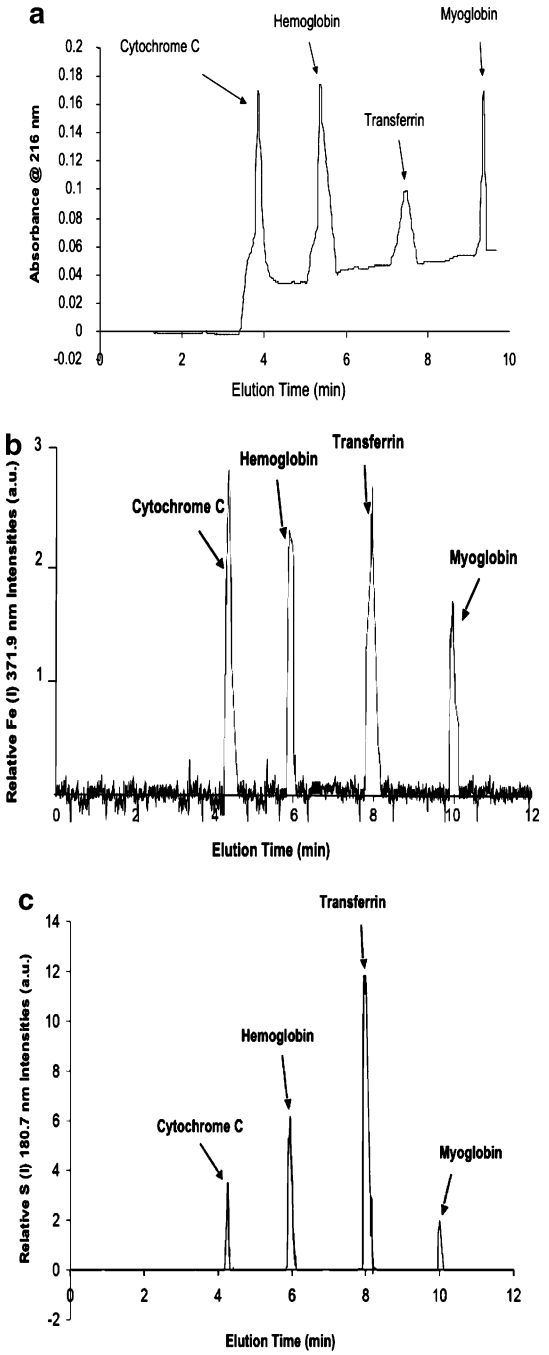

Figure 5. Separation of iron metalloproteins (1 mg/mL in protein) on PET C-CP fibers columns (a) 216 nm UV absorbance detection, (b) Fe (I) 371.9 nm, and (c) S (I) 180.7 nm detection by PB/HC−OES. PET C-CP column, gradient of 100:0 to 25:75 (water/acetonitrile) beginning at t = 2.5 min and terminating at t = 10 min, flow rate = 2 mL/min, nebulizer tip temp = 95 °C, nebulizer gas flow rate = ~800 mL/min, HC block temp = 235 °C, source pressure = 2 Torr of He, discharge current = 60 mA.

(63) Nelson, D.; Marcus, R. K. *Protein Pept. Lett.* **2006**, *13*, 95−99.

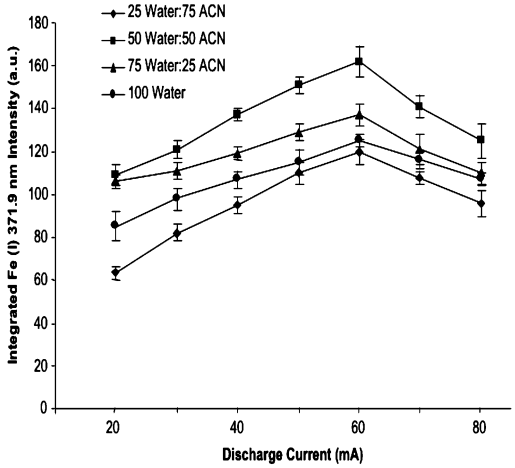

Figure 6. Effect of mobile phase composition on Fe (I) 371.9 nm emission intensity for triplicate injections of 200 μg/mL Fe in myoglobin. Injection volume = 50 μL, flow rate = 2 mL/min, nebulizer tip temp = 95 °C, nebulizer gas flow rate = ~800 mL/min, HC block temp = 235 °C, source pressure = 2 Torr of He.

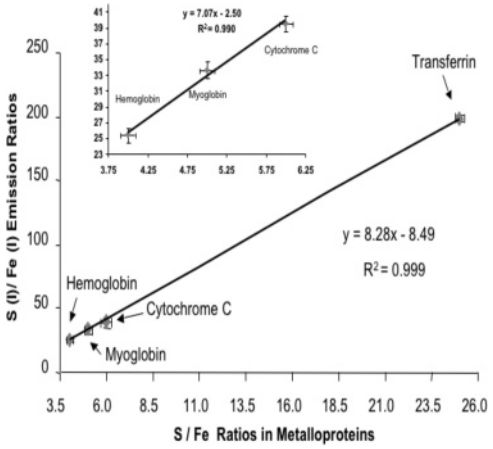

Figure 7. Comparison of experimentally obtained S (I) 180.7 nm/Fe (I) 371.9 nm emission intensity ratios to the actual atomic ratios (S/Fe) for the suite of Fe-metalloproteins. Error bars reflect propagation of errors in S (I) and Fe (I) measurements and resulting variance in composition.

Table 4. Quantitative Iron and Sulfur Recoveries in Metalloprotein Separations

protein	actual Fe conc μg/mL	peak area	peak area/ (μg/mL)
cytochrome *c*	4.1	25.3	6.1
hemoglobin	3.2	19.7	6.2
transferrin	4.9	29.6	6.0
myoglobin	2.6	17.6	6.7
protein	actual S conc μg/mL	peak area	peak area/ μg/mL)
cytochrome *c*	24.6	275	11.1
hemoglobin	51.2	553	10.8
transferrin	245	2458	10.0
myoglobin	13.2	153	11.6

composition on the Fe (I) responses was also performed across a range of discharge pressures. Here again, the 50:50 H_2O/ACN solvent yielded the highest response. The uniformity of these data is attributed to the efficient nebulization and particle desolvation afforded by the PB interface employed here.

One other important consideration in metal speciation studies is the uniformity of the resultant elemental response yields. Ideally, the elemental responses for the Fe and S analytes on a per-unit-mass basis would be independent of the protein identity and the eluting LC solvent composition. Table 4 presents the respective elemental concentrations and integrated optical emission responses for chromatograms of Figure 5, parts b and c. The final column presents the analytical recoveries for the two elements in units of integrated peak areas per unit concentration. As can be seen, the yields are indeed in excellent agreement, while the solvent composition is evolving from ~85:15 to 25:75 H_2O/ACN as the four proteins elute. The variation in the Fe (I) responses is just 7 % RSD, while that for S (I) is 8 % RSD. We are unaware of analogous comparisons in the ICP−OES/MS literature.

Fe-Metalloprotein Empirical Formula Determinations. The final step in the development of the LC−PB/HC−OES as a comprehensive speciation technique involves the multielement detection of signature elements present in the metalloprotein, including metals and nonmetals, which provide unique analytical responses. The basic approach here involved determining the empirical formulas of the various Fe-metalloproteins (Table 1) through the ratio of the measured emission intensities of the component elements Fe and S. Figure 7 illustrates this strategy for the simple case of combining the data obtained from the sulfur and iron response curves (Tables 2 and 3). Shown in this figure is the relationship between the ratios of S (I)/Fe (I) integrated emission intensities to the actual ratio of those elements in the suite of Fe-metalloproteins. As can be seen in the plot and corresponding regression data, the anticipated linear dependences hold true with a high degree of correlation ($R^2 = 0.999$), clearly demonstrating the system's ability to discriminate the identities of the metalloproteins based on multielement detection. Further improved accuracy would be expected in the case of simultaneous Fe (I) and S (I) detection. Even so, it is quite clear from these data that relatively small differences in stoichiometric composition can result in significant differences in the relative elemental responses.

While there are many works describing the potential use of elemental response ratios to discern protein identities, only the work of Hann et al.[23] does so for a number of proteins *and* in a chromatographic mode as illustrated here. ICPMS with dynamic reaction cell and sector field (e.g., high resolution) modes was evaluated following size exclusion chromatography separation. Fe/S ratios were determined using different means of internal standardization. The results obtained in a manner similar to those of Figure 7 resulted in empirical formulas with accuracies of 7.6−16.5% for myoglobin, hemoglobin, and cytochrome *c*. The errors in stoichiometry obtained here for the same set of proteins ranged from 7.8−8.9%. In both cases, the accuracy displayed would be quite sufficient to discern the identities of many metalloproteins.

CONCLUSIONS

The liquid chromatography−particle beam/hollow cathode−optical emission spectroscopy (LC−PB/HC−OES) system has been demonstrated to be a viable approach for the determination of Fe-metalloproteins. Evaluations of operating conditions demonstrated the need for high current densities and modest He gas

pressures for the detection of Fe (I) 371.9 nm in iron-containing metalloproteins. The nebulizer tip and HC temperature responses were assessed as tradeoffs between achieving effective vaporization and detrimental pyrolysis. The quality of the Fe (I) analytical response curves was evaluated over the iron concentration range of 0.1−100 μg/mL within the proteins with detection limits for triplicate injections down to the part-per-billion/nanogram levels of Fe. Quantification was also performed on the sulfur content of the same proteins based on S (I) 180.7 nm optical emission, with similar limits of detection, or slightly lower, than found for Fe. These figures of merit are very competitive with the aforementioned spectroscopic techniques with the distinct advantage of requiring very little sample manipulation and no spectrochemical interferences from atmospheric species. The reversed-phased HPLC separation involving high organic content was completed within a short time frame, suggesting that the detection method can be seen as an extension of the chromatography, rather than the detection method dictating the potential modes of chromatography. This is a key attribute of this methodology. The Fe (I) emission responses were seen to be fairly insensitive to the mobile phase composition, with both the Fe and S emission yields (peak area/concentration) being independent of the protein identity and HPLC solvent composition. Finally, the combination of reversed-phase metalloprotein separation with the possibility of empirical formula determination demonstrates the potential of the LC−PB/HC−OES as a simple, species-specific detector for metalloproteins in general.

ACKNOWLEDGMENT

Financial support from Savannah River National Laboratory, Aiken, SC, is gratefully appreciated.

Received for review August 15, 2006. Accepted January 15, 2007.

AC061516P